Computers & Geosciences 57 (2013) 32–43

Contents lists available at SciVerse ScienceDirect

Computers & Geosciences

journal homepage: www.elsevier.com/locate/cageo

# Computer-assisted mesh generation based on hydrological response units for distributed hydrological modeling

P. Sanzana [a,b,e,*], S. Jankowfsky [a], F. Branger [a], I. Braud [a], X. Vargas [b], N. Hitschfeld [c], J. Gironás [d]

[a] Irstea, UR HHLY (Hydrology–Hydraulics), 3bis Quai Chauveau, CP 220, 69336 Lyon Cedex 9, France
[b] Departamento de Ingeniería Civil, Facultad de Ciencias Físicas y Matemáticas, Universidad de Chile, Blanco Encalada 2002, Santiago, Chile
[c] Computer Science Department, Facultad de Ciencias Físicas y Matemáticas, Universidad de Chile. Av. Blanco Encalada 2120, Santiago, Chile
[d] Departamento de Ingeniería Hidráulica y Ambiental, Pontificia Universidad Católica de Chile, Av. Vicuña Mackenna 4860, Santiago, Chile
[e] Centro de Estudios Avanzados en Zonas Áridas (CEAZA), Raúl Bitrán s/n, Campus Andrés Bello, Colina El Pino s/n, La Serena, Chile

ARTICLE INFO

*Article history:*
Received 20 September 2012
Received in revised form
31 January 2013
Accepted 14 February 2013
Available online 26 February 2013

*Keywords:*
GRASS GIS
Hydrological response units
Distributed hydrological model
Computer-assisted mesh generation
Terrain representation

ABSTRACT

Distributed hydrological models rely on a spatial discretization composed of homogeneous units representing different areas within the catchment. Hydrological Response Units (HRUs) typically form the basis of such a discretization. HRUs are generally obtained by intersecting raster or vector layers of land uses, soil types, geology and sub-catchments. Polylines maps representing ditches and river drainage networks can also be used. However this overlapping may result in a mesh with numerical and topological problems not highly representative of the terrain. Thus, a pre-processing is needed to improve the mesh in order to avoid negative effects on the performance of the hydrological model. This paper proposes computer-assisted mesh generation tools to obtain a more regular and physically meaningful mesh of HRUs suitable for hydrologic modeling. We combined existing tools with newly developed scripts implemented in GRASS GIS. The developed scripts address the following problems: (1) high heterogeneity in Digital Elevation Model derived properties within the HRUs, (2) correction of concave polygons or polygons with holes inside, (3) segmentation of very large polygons, and (4) bad estimations of units' perimeter and distances among them. The improvement process was applied and tested using two small catchments in France. The improvement of the spatial discretization was further assessed by comparing the representation and arrangement of overland flow paths in the original and improved meshes. Overall, a more realistic physical representation was obtained with the improved meshes, which should enhance the computation of surface and sub-surface flows in a hydrologic model.


## 1. Introduction

Distributed hydrological models represent the catchment heterogeneity in an explicit way. Thus, a discretization leading to homogeneous and representative spatial units becomes relevant to solve the equations describing the physical processes involved. Pixels in a grid-cell representation are the elementary spatial units mostly used by many models such as the Système Hydrologique Européen model (Abbott et al., 1986a, 1986b) or TOPMODEL (Beven and Kirkby, 1979) to represent spatial information. Other models consider a vector objects representation in which a non-uniform mesh of elementary irregular units is defined. The Hydrological Response Unit (HRU), a concept proposed by Flügel (1995), is an example of these elementary units. HRUs possess unique land uses, soil attributes and flow routing properties, which are derived from intersecting polygon layers representing information such as land use, soil type, sub-catchments and geology. Polyline layers corresponding to natural and artificial drainage elements can typically be combined with a HRU representation. Thus, the resulting hydrological mesh is formed by simple polygons with very irregular shapes, which are more suitable for representing man-made features that significantly affect hydrological processes in a catchment (Lagacherie et al., 2010). This is particularly relevant for suburban and urban catchments, in which artificial elements (i.e. sewers, channels and streets) can modify significantly the flow directions (Gironás et al., 2009). Some of the distributed hydrological models based on a HRU representation include PRMS (Flügel, 1995; Bongartz, 2003), SWAT (Arnold et al., 1998), J2000 (Krause, 2002), MHYDAS (Moussa et al., 2002), PREVAH (Viviroli et al., 2009), and models built within the LIQUID modeling framework (Branger et al., 2010).

For the determination of non-uniform meshes of elementary units, Dehotin and Braud (2008) proposed a three level discretization methodology: (i) Catchment sub-divided into sub-catchments,

* Correspondence to: Mailbox: Casilla 599, Correos de Chile.
Tel.: +56 51 204378; fax: +56 51 334874.
*E-mail addresses:* pedro.sanzana@ceaza.cl, psanzana@ing.uchile.cl (P. Sanzana).

0098-3004/$ - see front matter © 2013 Elsevier Ltd. All rights reserved.
http://dx.doi.org/10.1016/j.cageo.2013.02.006

(ii) sub-catchments discretized into hydro-landscapes (e.g. HRUs) where hydrological processes are homogeneous, and (iii) hydro-landscapes further adapted to fulfill numerical constraints. This paper addresses this third level and some aspects of the second level.

Several GIS tools have been developed to delineate HRUs, including GRASS-HRU (Schwartze, 2008), Geo-MHYDAS (Lagacherie et al., 2010), WINHRU and GRIDMATH (Viviroli et al., 2009), and AVSWAT (Di Luzio et al., 2004). However, vector based HRU model meshes come also with specific constraints. Special considerations regarding topological and geometric characteristics of the HRUs are needed to obtain stable and meaningful numerical solutions. The three main issues to be addressed when defining HRUs are as follows:

1. Cleaning of polygon geometry and topology to deal with
   (a) The direct overlay of several digitized polygons or lines layers can create small artificial non-representative units, which play no role in representing the terrain and must be dissolved. As an example Fig. 1a shows an isolated small artificial unit generated near a major unit (Fig. 1b). When numerous, these units can increase the computation time.
   (b) Digitalization of raster images can create polygons with many right angles representing the size of the grid cell. The length of the polygon boundary, often used for calculating wetted sections in overland and subsurface flow, becomes longer in this case. Hence, the perimeter of these polygons should be smoothed to avoid overestimation of boundary lengths (Fig. 1b).
   (c) Polygon intersections can create holes inside the HRUs, generating numerical indefinition in the hydrological model (Fig. 1d). These units must be partitioned to avoid the generation of these holes and properly connect HRU's to ensure continuity in the model.
2. Improving the property homogeneity within a model unit. Topography partly controls water fluxes within a watershed and influences many aspects of the hydrologic system (Wolock and Price, 1994). Thus, raster based information, such as elevation or slope, is of interest for simulating hydrological processes. As this information is not initially included in the HRUs definition, these properties may not be homogeneous enough within a given HRU, and further segmentation may be necessary to get more homogeneous units.
3. Improving the mesh geometry for a better numerical stability. Land use objects, such as forest stretches, hedgerows, agricultural fields or urban cadastral units do not always have convex geometries. Furthermore, the overlay of different property layers can create bad-shaped polygons with thin geometries (Fig. 1b) or polygons with their centroid outside of their boundary (Fig. 1c). This may cause problems when defining the topology of flow routing from one HRU to another. Typically, the distance between the centroids of the polygons and their boundaries is used to calculate flow path lengths among HRUs and overland and subsurface flows. This distance has no realistic meaning if the centroid is outside of the polygon, and a modification of the HRUs becomes necessary. Finally, HRUs can greatly vary in sizes, which can affect flow routing and the stability of numerical schemes. Thus, the segmentation of very large polygons is recommended to obtain a more homogeneous model mesh.

Cleaning tools available in most GIS software can solve the first category of issues. To address situation 1a in GRASS Development Team (2011), Schwartze (2008) used raster pixel-dissolving functions and generated vector HRUs using a raster-to-vector conversion. Alternatively, Lagacherie et al. (2010) developed enhanced dissolving tools for vector data in GeoMHYDAS, which are specific to HRUs. Problem 1b can be solved using specific GIS functions such as the m.douglas tool (Lagacherie et al., 2010), based on the Douglas–Peucker algorithm (Douglas and Peucker, 1973), or the Snakes algorithm (Kass et al., 1988) of the function v.generalize in GRASS. Problem 1c must be addressed with a segmentation approach. Most common partition algorithms transform polygons into simpler polygons such as trapezoids or triangles. However these algorithms increase the number of final polygons and the mesh units become physically meaningless.

The second category of issues relates to the heterogeneity typically represented by raster data. The grid resolution must be small enough to describe this variability (Seyfried and Wilcox, 1995), particularly if this is significant. For example, Zhang and Montgomery (1994) found that a 10 m grid resolution allowed a good compromise between the quality of the terrain representation and data volume for simulating physical processes. To analyze terrain heterogeneity GRASS has comprehensive tools described by Hofierka et al. (2007). TOPAZ uses automated analysis of digital landscape topography in raster scheme, as described by Garbrecht and Martz (1997). However, these tools cannot be applied to analyze raster-based terrain properties within polygons derived from vectorial layers.

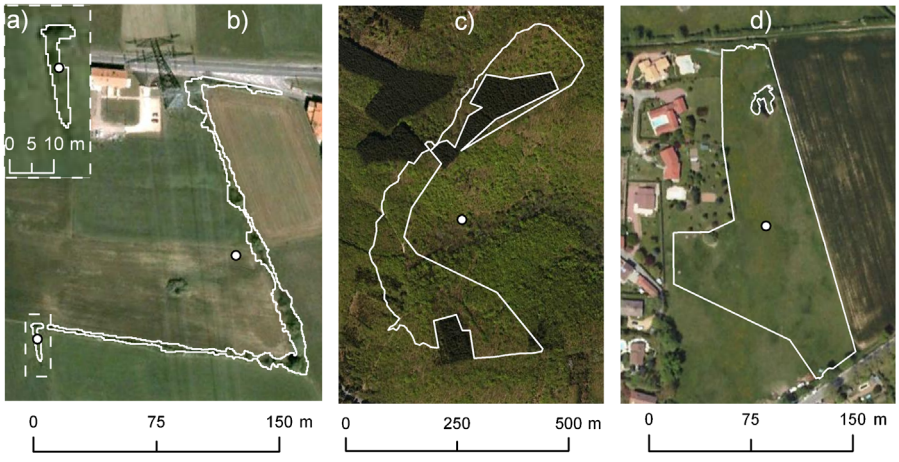


**Fig. 1.** Typical bad-shaped polygons for a 2D hydrological mesh: (a) non-representative small area, (b) bad-shaped polygon with a thin geometry in which the perimeter is overestimated, (c) concave unit with its centroid outside the boundary and (d) a polygon with hole inside.

The third category of issues is more complex. Lagacherie et al. (2010) proposed an algorithm for sliver areal features, which dissolve thin polygons with their neighbors. Sometimes this approach is not desirable, as the bad-shaped polygon may correspond to a relevant hydrological object. An alternative approach is to sub-discretize the HRUs into Triangular Irregular Networks (TINs) (Bocher and Martin, 2012). TIN meshes are well adapted to numerical solutions of differential equations, and are used in comprehensive hydrological models such as InHM (VanderKwaak and Loague, 2001) or tRIBS (Ivanov et al., 2004). This approach also increases the number of model units, and the physiographical character of the mesh also gets lost.

The objective of our study was to generate an HRU model mesh compatible with numerical criteria and homogeneity requirements. We developed mesh generation computer assisted tools addressing the problems mentioned above, focusing more specifically on problems listed in categories 2 and 3. Although our work is a contribution to the development of the hydrologic peri-urban PUMMA Model (Jankowfsky et al., 2010, Jankowfsky, 2011), built within the LIQUID modeling framework (Branger et al., 2010), the concepts and methods involved are also relevant for other distributed hydrological models. These methods and concepts can be applied to models in which interconnected HRUs are generated from objects typically found in periurban catchments, such as urban cadastral units, agricultural fields and forests, and artificial and natural drainage systems. A central objective in our development is to better represent overland and subsurface flow paths, as well as interactions with the natural and artificial drainage network. This improvement allows the understanding and quantification of runoff contributions from a variety of HRU's to the different components of drainage networks.

## 2. Materials and methods

In this section, we first review the data preparation methods to obtain clean and topologically consistent GIS layers. Then the following new methods to improve the model mesh are presented in detail: (1) segmentation of polygons with high variability of a given property, (2) removal of bad-shaped polygons, and (3) segmentation of very large polygons. Finally, we present the case study catchments used to test the proposed methods.

We developed several Python (Python Software Foundation, 2011) scripts to implement these new methods (Table 1). The scripts include GRASS GIS functions, as GRASS is the only free open-source GIS software with topological functionalities (Branger et al., 2012). Additional softwares, such as Triangle (Shewchuck, 1996) and R (R Development Core Team, 2011), were also used to get fast and high quality triangulation of bad-shaped polygons. The developed tools are computer-assisted because, although they strongly rely on computer coding, the modeler must still provide critical information such as threshold values, ranges and specific quantities for the complete execution. Similar computer algorithms in which the user must provide specific information are widely used. For example, threshold values for contributing areas are needed for channel identification in DEM's when using tools such as r.watershed in GRASS or Arc-Hydro in Arc-GIS (Olivera et al., 2002). Furthermore, quantity and ranges of slope, aspect and height contours are required in the overlapping delineation processes proposed by Schwartze (2008) to generate HRUs. Finally, the segmentation procedure implemented in GeoMHYDAS (Lagacherie et al., 2010) requires a minimum area to dissolve neglected and sliver units.

### 2.1. Data preparation and cleaning of GIS layers: smoothing and partition of polygons with holes

Typically a pre-processing is required before each segmentation task to obtain "clean" layers. For the smoothing of boundaries, the Douglas–Peucker (Douglas and Peucker, 1973) and Snakes (Kass et al., 1988) algorithms were assessed. Two implementations of the Douglas–Peucker algorithm are available in GRASS: the command v.generalize and the script m.douglas (Rabotin, 2010).

The intersection of different layers can lead to polygons inside external polygons, referred as to holes, which are undesirable for spatial modeling as they can distort flow paths. The implemented algorithm (*polygons_holes.py* in Table 1) subdivides all polygons with holes to generate new sub-sets of polygons without them (Fig. 2). The algorithm first identifies the shortest distance from each vertex of the inner polygon to the outer polygon ($w$, $x$, $y$ and $z$ in Fig. 2). Then the shortest and longest distances, $x$ and $z$, are used to generate the polylines to split the outer polygon and transform the hole in a new polygon.

### 2.2. Segmentation of polygons with high variability of a raster-based property: application with slope criterion

For hydrologic modeling, it is desirable to incorporate some raster-based properties not included in the initial HRU delineation. An example of such property is the slope, which is typically available in a grid-cell representation, and affects different relevant hydrological processes. Hence, a further segmentation process is necessary to disaggregate highly heterogeneous HRUs into

**Table 1**
Summary of the different tasks and scripts developed.

| Task | Description | Script developed |
|---|---|---|
| Partition of polygons with holes | ***Data preparation and cleaning of GIS layers:*** Split polygons and create a new subset without holes. | Polygons_Holes.py |
| Integration of raster based properties into polygons | ***Segmentation of polygons with high variability of a raster based property:*** Segmentation with Inter Quartile Range (IQR) boundaries and small area dissolving. Final smoothing with Snakes algorithm and reduction of vertexes with Douglas algorithm. | Slope_Segmentation.py |
| Convexity Segmentation | ***Removal of bad-shaped polygons:*** Triangulation with Software Triangle. Exporting and Importing GRASS ASCII into POLY format with R Script. Dissolving rule with Convexity Index criterion. | Convexity_Segmentation.pyAscii2Poly.r Triangle2Ascii.r |
| Area Segmentation | ***Segmentation of too large polygons:*** Idem to Convexity Segmentation but with additional restriction of maximum area in initial triangulation. Dissolving Rule with Convexity Index and Area restriction. | Area_Segmentation.py |

*Note:* Scripts can be requested to author's email address: pedro.sanzana@ceaza.cl, or co-authors: flora.branger@irstea.fr, isabel.braud@irstea.fr.

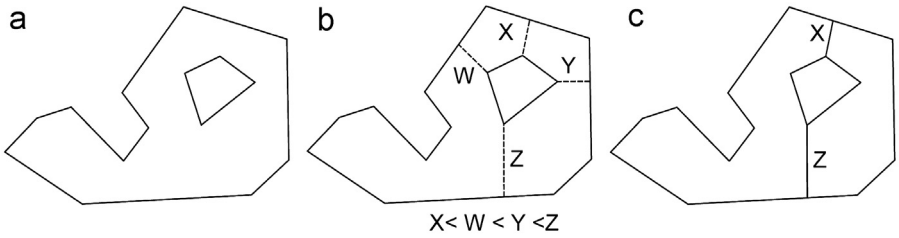


**Fig. 2.** Partition of polygons with holes. (a) Initial polygon, (b) nearest distances from the vertexes of the inner polygon and (c) split lines: maximum ($x$) and minimum ($z$) distances.

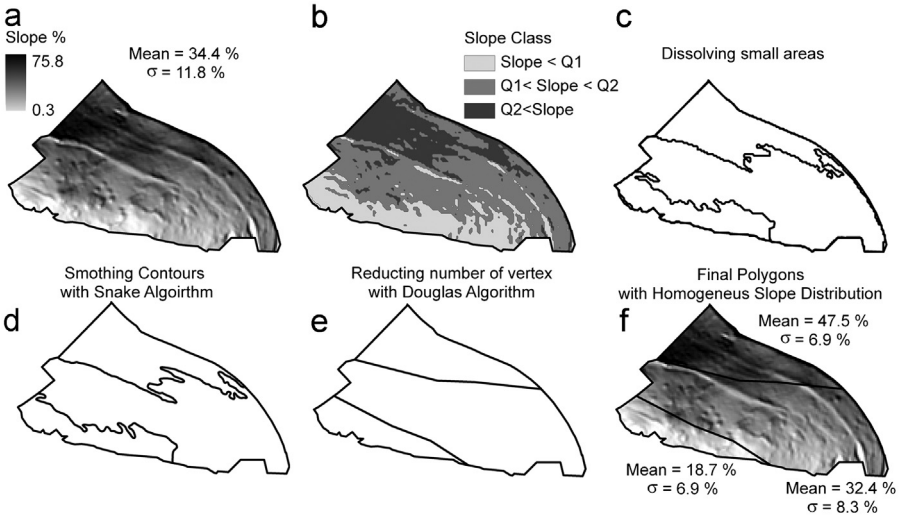


**Fig. 3.** Segmentation of a polygon with a raster-based highly variable property. Slope is used in this example with STD threshold of 10.

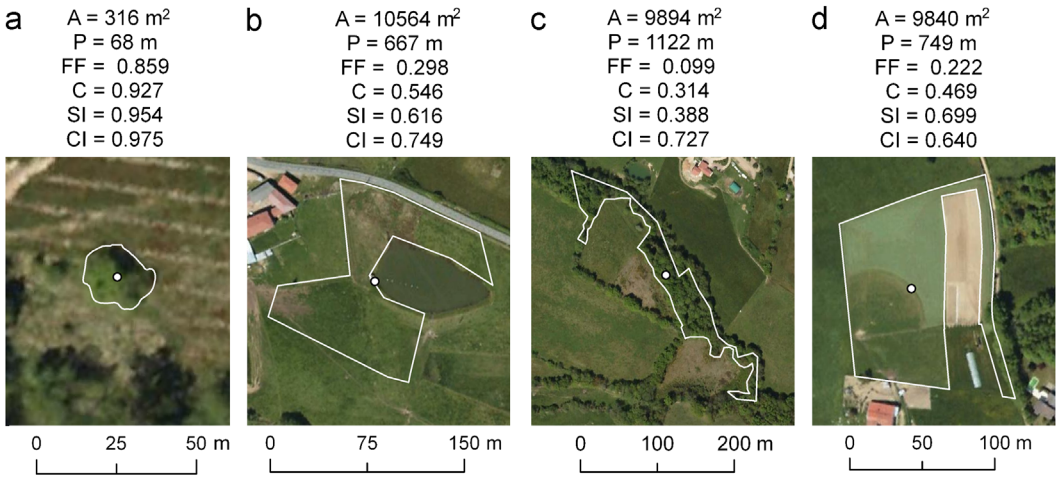


**Fig. 4.** Different types of possible HRUs and corresponding values of area ($A$), perimeter ($P$) and shape descriptors ($FF$, $C$, $SI$ and $CI$).

regions with homogeneous features. For this purpose, we used a threshold value of the standard deviation of the property ($\sigma_T$). For values of standard deviation $\sigma > \sigma_T$, segmentation is performed. The threshold could also be defined in terms of the coefficient of variation, in order to compare polygons with different mean values of the property. However, by using $\sigma_T$ one can control the allowable dispersion within each polygon. To define the boundaries delimiting homogeneous property areas within the different HRUs, we used the Inter Quartile Range (IQR), a statistical parameter defined as the difference between the third and first quartiles (Q3) and (Q1). The segmentation procedure is defined in details in Appendix A1 and illustrated in Fig. 3 using the slope as the raster-based property.

### 2.3. Segmentation of concave units

The flowpath length between HRUs is given by the distance between their geometric centroids. Hence, this distance must be representative of the trajectory to get a realistic physical description of the flow. Therefore the partition of bad-shaped polygons becomes necessary to obtain convex or pseudo-convex polygons with their geometric centroid located within them.

Well-shaped polygons (Fig. 4a) facilitate the definition of a meaningful length in contrast to bad-shaped polygons (Fig. 4b–d). The identification and correction of these polygons is then required. Different shape descriptors proposed by Russ (2002), such as the Form Factor ($FF=(4\pi A)/P^2$), Compact ($C=\sqrt{4\pi A}/P$), Solidity Index ($SI=A/A_{Convex}$) and Convexity Index ($CI=P_{Convex}/P$), can be used for identifying well- and bad-shaped polygons. In these descriptors, $P$ and $A$ are the perimeter and the area of the polygon, and $P_{Convex}$ and $A_{Convex}$ are the perimeter and the area of the convex hull polygon containing the polygon of interest. The convex hull area is the minimal convex area in which any line between two inner points is completely contained within the polygon. A convex polygon always has its geometrical centroid inside and can be considered as a well-shaped unit.

Each descriptor characterizes different geometrical features (Fig. 4). For example, *FF* and *C* are sensitive to thin units (i.e. values of these descriptors decrease for $A \ll P$), whereas *CI* and *SI* are sensitive to concave polygons, focusing on the perimeter and the area respectively. *SI* is inversely proportional to the convex-hull area, as shown in Fig. 4b ($SI=0.616$) and Fig. 4c ($SI=0.388$). As *CI* detects best concave polygons (i.e. polygon in Fig. 4d), a Convexity Index Threshold (*CIT*) was chosen for the identification of the polygons requiring correction. Values of $CI < CIT$ are associated with bad-shaped polygons that must be corrected.

Some algorithms are available for partitioning polygons into convex pieces, with the triangulation being the simplest one, although non-optimal in terms of the number of convex pieces generated (O'Rourke, 1998). The Hertel and Mehlhorn algorithm (Hertel and Mehlhorn, 1983) provides a simple and fast solution that does not minimize the number of pieces. It arbitrarily triangulates the polygon and deletes the diagonal to generate only convex polygons. On the other hand, the Greene Algorithm (Greene, 1983) available in the CGAL Library (CGAL, 2011) generates the minimum number of pieces, but is more time consuming (O'Rourke, 1998). With both algorithms, the number of final pieces depends on the number of vertexes of the input polygons, and computation cost can become a relevant issue both in the generation of the improved mesh and the subsequent hydrologic modeling.

The GRASS function v.delaunay creates a Delaunay triangulation from an input vector map, although it is not a robust implementation and works only with convex polygons. Hence, our solution considers first a Delaunay triangulation using the *Triangle* Software (Shewchuck, 1996) which can address concave or convex polygons, with or without holes. Second, we dissolve adjacent triangles based on a chosen value of the *CIT* (Fig. 5) to decrease the number of polygons and improve the physical meaning of each unit of the model mesh. The dissolution rule takes into account the *CI* with a hierarchical area order. Triangles are dissolved so that the *CI* values of all new generated polygons equal or exceed the *CIT* value. The convex segmentation procedure is defined in Appendix A2 and illustrated in Fig. 5 using a *CIT* value of 0.95. The final number of pseudo-convex pieces depends on the *CIT* value. For instance, in the example of Fig. 5, the number of final pieces decreases to 2 when *CIT* equals 0.90.

### 2.4. Segmentation of very large polygons

Large polygons generate numerical problems when connected to small polygons. This can affect the calculation of flow paths, water fluxes, ponding levels or water table levels. All the polygons with an area exceeding a threshold value defined by the user are segmented with the same procedure used for the convexity segmentation that considers a maximum triangle area in the triangulation.

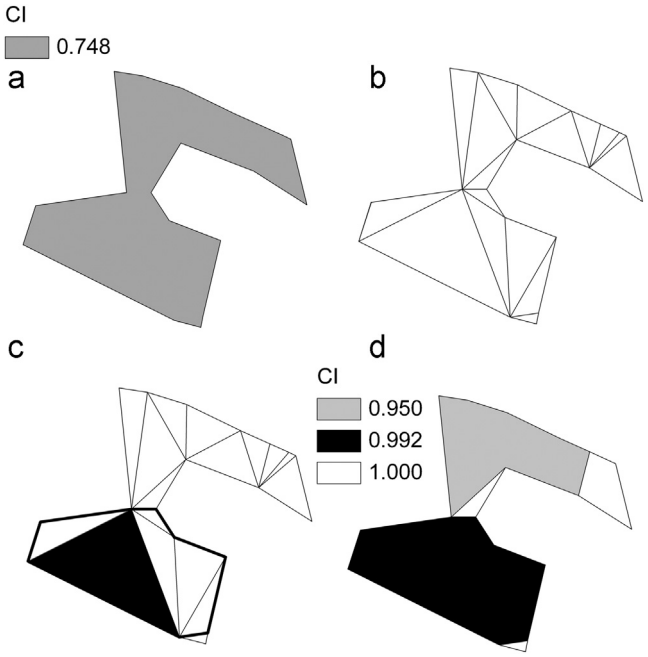


**Fig. 5.** Scheme of Convex Segmentation: (a) initial polygon, (b) triangle output, (c) selection of neighbor triangles grouped with CIT ≥ 0.950 and (d) dissolved polygons.

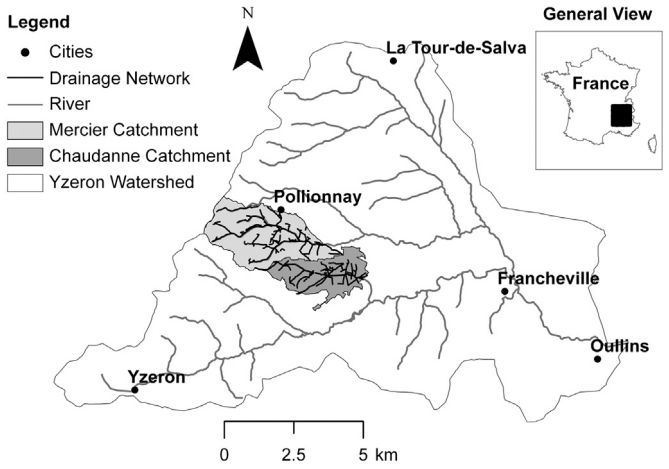


**Fig. 6.** The Yzeron watershed and the Mercier and Chaudanne subcatchments.

### 2.5. Case study

The computer-assisted mesh generation tools were tested in two subcatchments within the Yzeron peri-urban watershed (150 km$^2$) located south west of Lyon, France (Fig. 6). The Mercier subcatchment (7 km$^2$) is covered with forests, crops and urban areas (about 10%), while the Chaudanne subcatchment (4.1 km$^2$) is covered by a mix of crops (45%) and urbanized areas (53%) (Braud et al., in press). Given that most of the issues previously depicted are typically related to polygons generated in rural areas, we focused our analysis on the Mercier catchment. Nonetheless we also provide some representative statistics for the Chaudanne catchment.

HRUs were delineated from several maps including a detailed land use map obtained by manual digitalization (Jacqueminet et al., in press), a pedology map produced by the Soil Information of Rhône-Alpes as part of the Soil Management, Conservation and Inventory program (IGCS, 2013), a geology map (BRGM, 2013),

a 2 m resolution Digital Elevation Model (DEM) derived from a Lidar (Light Detection And Ranging) survey (Sarrazin, 2012), a subcatchment map derived using the method proposed by Jankowfsky et al. (2012), maps of the ditch network (Jankowfsky et al., 2012), as well as sewer maps, which were provided by the local sewer system manager SIAHVY (Syndicat Intercommunal pour l'Aménagement de la Vallée de l'Yzeron). The HRU map derived from the rough intersection of all these layers is shown in Fig. 7a.

## 3. Results

This section describes the results obtained when applying each of the steps of the improvement procedure previously described, as well as the issues found in generating the physiographical representation for the study subcatchments. Although not compulsory, we recommend applying these steps in the same order as shown. Jankowfsky (2011) provides more details and results when using the proposed sequence in the Mercier and Chaudanne catchments.

### 3.1. Data preparation and cleaning of GIS layers

One of the main problems detected at initial stages was the non-representative shapes of areas with vegetation, whose extraction is affected by the low resolution of the corresponding raster images. Thus, the perimeter of these shapes is originally overestimated (Fig. 8a). After trying both the Douglas–Peucker algorithm (Fig. 8b) and Snakes algorithm (Fig. 8c), we concluded that the last produces a more realistic representation and reduces the initial perimeter in about 25%.

A second issue addressed at early stages was that of the holes within polygons. They were successfully segmented using the *polygons_holes.py script,* 10 in the Mercier and 11 in Chaudanne catchment. Fig. 9a and b shows two HRUs partitioned to avoid the holes produced by two different vegetal features. Fig. 9c shows a HRU partitioned to avoid the hole produced by a greenhouse.

### 3.2. Segmentation of polygons with high variability of a given property

We applied the proposed algorithm for the slope map of the Mercier catchment, which was obtained from the DEM using the r.slope function in GRASS. After a visual inspection of the Mercier HRUs, we chose a $\sigma_T$ value of 6% for the slope. Fig. 3f shows the results obtained after applying the segmentation script *slope_segmentation.py* (Table 1). The IQR criterion generated new polygons whose boundaries had right angles. The subsequent application of the Douglas–Peucker and Snakes algorithms allowed reducing the vertexes and smoothing the contours, respectively. 42 polygons were segmented into 133 final pieces in the Mercier catchment. As a result the area covered by HRUs with high standard deviation was reduced from 93.4 ha to 51.6 ha, that means a reduction of 13% to 7% of the total area.

Furthermore, the integration of raster based properties into polygons allows segmenting units with a high standard deviation and creating new units. The final standard deviations of the new units depend on the spatial distribution of the parameter selected. Thus the script reduces the area covered by units with non-homogeneous distribution, but this does not assure that all the output units preserve a standard deviation less than the threshold (i.e. Maximum Standard deviation of Slope increase to 14.25 in Table 2). A possible solution to assure a reduction of the maximum value would be continuing segmenting in an iterative way, but this

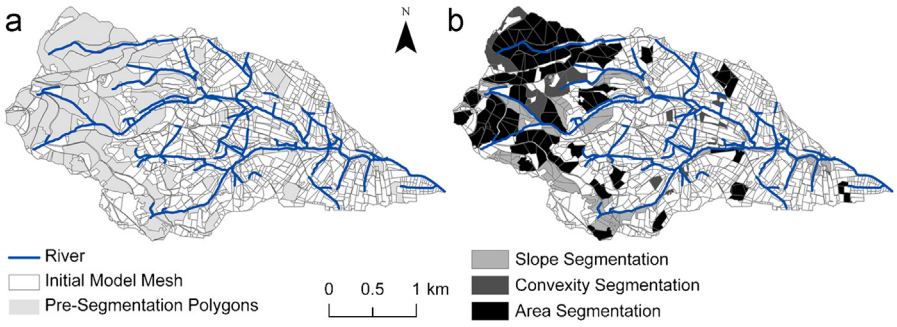


**Fig. 7.** The Mercier catchment: (a) initial mesh and (b) improved mesh.

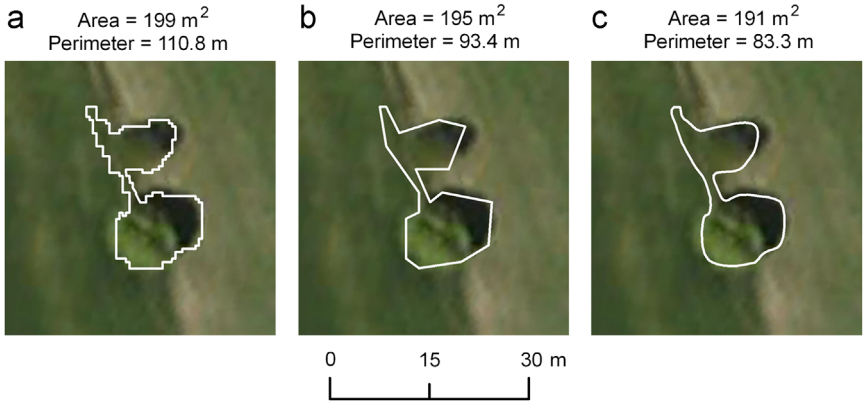


**Fig. 8.** Representation of a green area in the Chaudanne catchment: (a) raw representation, (b) representation after Douglas–Peucker algorithm, and (c) representation after Snakes algorithm.

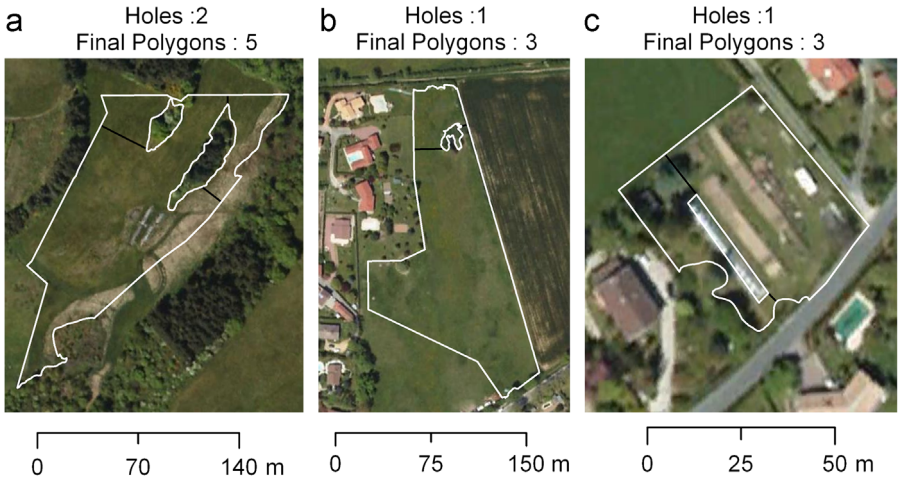


**Fig. 9.** HRU's examples from the Chaudanne catchment: (a) two holes produced by green areas, (b) one hole produced by green area, and (c) one hole produced by a manmade feature.

**Table 2**
Main statistics of area, standard deviation and convexity index in the Mercier catchment for the initial and enhanced mesh.

| Statistical parameter | Area $_{Initial}$ ($m^2$) | Area$_{Optimized}$ ($m^2$) | $\sigma_{Initial}$ (%) | $\sigma_{Optimized}$ (%) | $CI_{Initial}$ | $CI_{Optimized}$ |
|---|---|---|---|---|---|---|
| Average | 3289 | 2899 | 3.09 | 3.14 | 0.969 | 0.974 |
| Median | 834 | 945 | 2.58 | 2.64 | 0.990 | 0.991 |
| Min | 2 | 10 | 0.12 | 0.12 | **0.599** | **0.752** |
| Max | **192,144** | **24,595** | 13.98 | 14.25 | 1.000 | 1.000 |
| Std | 8270 | 4461 | 2.16 | 2.18 | 0.052 | 0.040 |

might result in very small units depending on the quality of the raster resolution. Overall, this segmentation method uses simple steps and produces satisfactory results, comparable to those generated by other more sophisticated methods (Klingseisena et al., 2008, Taylor et al., 2009), which can be also explored to potentially improve the resulting shapes from our method.

### 3.3. Segmentation of bad-shaped polygons

Polygons with *CI* less than a certain *CIT* were considered as bad shape units not suitable for modeling. Values of *CIT*=0.75 and 0.88 were adopted for the Mercier catchment and the Chaudanne catchment, respectively. We chose different *CIT* values because of the available land-use maps. In the Chaudanne catchment the vegetation extracted from raster maps had a more detailed perimeter than in the Mercier catchment, for which the land use map was determined manually. Therefore, meshes with sinuous HRUs required a larger *CIT* value in order to obtain well-shaped elements. The convexity segmentation procedure previously depicted was applied to all the HRUs using these *CIT* values. 20 polygons within the Mercier catchment were modified. Fig. 10 illustrates some polygons for which a correction was needed, together with the final result. Fig. 10a shows a HRU in the Mercier catchment partitioned into pseudo convex units with the centroids completely inside of new ones. Fig. 10b shows a HRU located near the riverside, in which the final units get more regular pieces with a *CI* larger than 0.75. Finally, the resulting polygons in Fig. 10c shows that the segmentation process is capable of detecting and segmenting conflictive objects such as "hedges". The *CI* values of all the polygons to be segmented in the Mercier catchment ranged between 0.59 and 0.74. Based on our results, we propose values of *CIT* of 0.75 and 0.88 for simple and detailed meshes respectively.

### 3.4. Segmentation of very large polygons

26 polygons in the Mercier catchment exceeded an area of 2 ha, the threshold value adopted for the area segmentation. For this process we first subdivided polygons with areas larger than this threshold into TIN's (see Fig. 11a). Then, the routine *Area_segmentation.py* (Table 1) dissolved the triangles using the convexity criterion and the area restriction. After dissolving 165 triangles, we ended up having 17 final homogeneous polygons (Fig. 11b), all of them with similar areas and a *CI* larger than 0.95, which facilitates running a hydrological model afterwards.

### 3.5. Thresholds and parameter selection to apply GIS tools

The developed computer assisted tools require the definition of the following critical values: (1) In data preparation and cleaning of GIS layers, we selected values of the Snakes elasticity ($\alpha$=1.0) and stiffness ($\beta$=1.0), as well as a 50% of points reduction in the Douglas algorithm; (2) threshold values ($\sigma_T$) for the standard deviation of properties highly variable within polygons, to separate them into more uniform units. Particularly, for the slope we selected a value of $\sigma_T$=6.0%; (3) a critical value of the convexity index for the triangulation-dissolution process to remove bad-shaped polygons (i.e. values of 0.75 and 0.88 for simple and detailed meshes respectively); (4) a maximum polygon area (2 ha in the case of the Mercier catchment) to generate a mesh of more homogeneous elements when large polygons due to forest stretches and low urbanization occur.

### 3.6. Final improved mesh

Overall, the mesh improvement produced more HRUs of smaller size, which are more homogeneous and representative of the physical properties within the catchment (see Fig. 7b for the Mercier Catchment). In total, 117 polygons (38.3% of the total catchment area) were treated in the Mercier catchment (i.e. 8 to remove holes, 43 for homogeneity of slopes, 20 to improve convexity, and 46 to reduce area). Thus, the final number of polygons increased from 2208 to 2518 in Mercier (14.0%), and from 2573 to 2945 in Chaudanne (14.4%). For the case of the

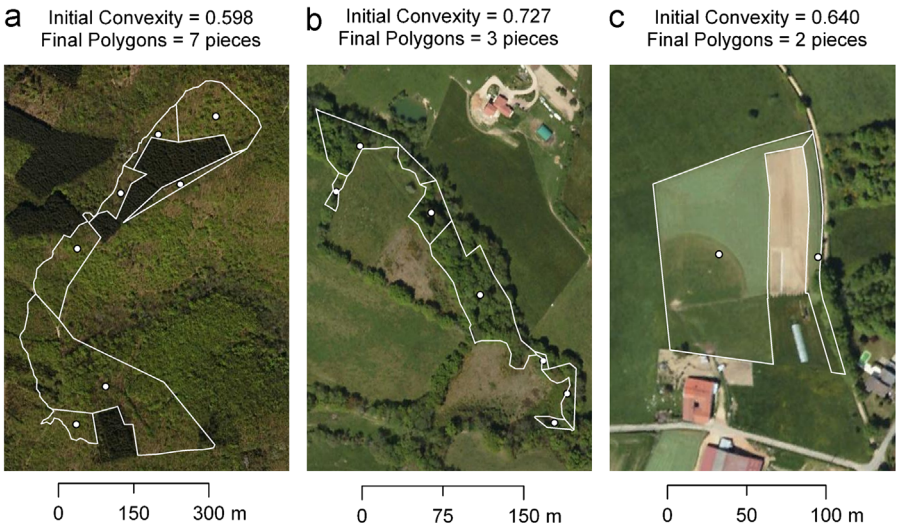


**Fig. 10.** Examples of HRUs segmented using a $CIT=0.75$.

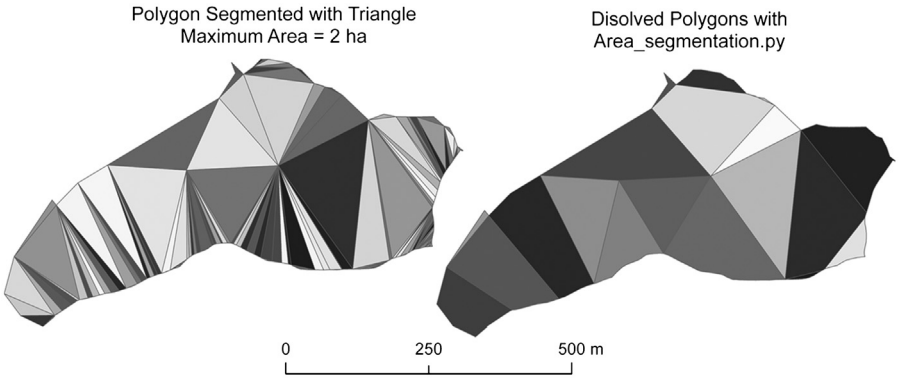


**Fig. 11.** Example of segmentation of very large polygons: (a) triangulated large polygon: 19.2 ha, and (b) dissolved homogeneous polygons with CIT $\geq$ 0.95 and area $\geq$ 2 ha.

Mercier catchment, Table 2 shows a reduction in the range of area values, the standard deviation and the mean value for the improved mesh. The minimum value of the *CI* before the improvement ($CI=0.599$) significantly increases to a value of $CI=0.752$. Although the average and median values of *CI* changed slightly, the standard deviation of the *CI* values reduced about 20%. Furthermore, the segmentation of the 43 elements with high standard deviation of slope into 133 elements, reduced from 93.4 ha to 51.6 ha the area covered by polygons with highly variable slope (i.e. from 13% to 7% of the total catchment area). Hence, although the maximum standard deviation increases from 13.98% to 14.25% in a HRU unit, the total area of HRUs with nonhomogeneous representation of slope decreased in 45%. The larger number of polygons in the improved mesh is still compatible with reasonable computing times. The improvement in terms of quality and representation of the HRUs allows obtaining a model mesh more suitable for hydrological modeling.

## 4. Discussion and interest in terms of hydrological response

The arrangement of the flow paths from the points in the basin to its outlet is of the most crucial importance when studying the structural characteristics of a drainage network, and its implications on the hydrologic response (Rodriguez-Iturbe and Rinaldo, 1997). This is also true for urban catchments (Lhomme et al., 2004; Rodriguez et al., 2003; Rodriguez et al., 2005; Gironás et al., 2007; Gironás et al., 2009; Gironás et al., 2010; Meierdiercks et al., 2010; Rodriguez et al., 2012). Thus, we assessed the effect of the mesh improvement on the generated flow paths by comparing the initial and segmented meshes visually, and by means of the so called width function.

First, we examined the effect of the segmentation procedure on the flow paths linking the polygons. These paths were obtained using the OLAF module (Brossard, 2011, Jankowfsky, 2011), which routes the flow between HRUs and the drainage network following topography towards the lowest neighbor HRU or drainage reach. Fig. 12 illustrates some of the major changes both in the extension and trajectory of the flow paths. For example, in the pre-segmented mesh (Fig. 12a), point *a* drains to the stream through point *b*, located north of the stream, which receives contributions from other 3 units. On contrary, a more realistic representation is obtained in the segmented mesh (Fig. 12b), where the flow path starting at the same unit (point $\underline{a}'$) crosses units $\underline{b}'$ and $\underline{c}'$ before reaching the river at point $\underline{d}'$. In this case, units $\underline{b}'$ and $\underline{c}'$ are located south of the river. Overall, a denser and potentially more representative network of overland flow paths is observed in the improved mesh, in which the number of HRU's and connections increases (Fig. 12). Indeed, the drainage density of overland flow paths (i.e. the ratio of the total length of the

paths connecting the HRUs to the catchment area) increased from 19.9 km/km$^2$ for the pre-segmentation network to 22.4 km/km$^2$ for the post-segmentation network.

We also used the width function $W(x)$ for assessing the effects of segmentation on the organization of the flow paths. $W(x)$ is defined as the number of links at a distance $[x, x+\Delta x]$ from the outlet through the drainage network. The linkage between the spatial structure of the basin and its hydrological response is embedded in $W(x)$, because the travel time from each point in the basin is related to the flow velocity and the flow distance that must be covered (Rodriguez-Iturbe and Rinaldo, 1997). $W(x)$ has previously been used to compare drainage network representations (Richards-Pecou, 2002; Moussa, 2008; Rodriguez et al., 2012), and to assess urbanization effects on the drainage network structure and potential impacts in the resulting hydrograph response (e.g., Smith et al., 2001; Gironás et al., 2009; Ogden et al., 2011). Thus, we used $W(x)$ to determine the possible impact of the segmentation procedure in the representation of overland flow paths.

We compared $W(x)$ obtained before and after the mesh segmentation ($W_{pre\text{-}s}(x)$ and $W_{post\text{-}s}(x)$, respectively), using a value of $\Delta x = 20$ m (Fig. 13a). Our objective was not to quantify the hydrologic effect of the segmentation (a hydrologic model is also required), but to show the effect of different HRU segmentations on the overland flow representation and the generated drainage network. Different networks would have a potential impact on the simulated hydrologic response (i.e. different drainage networks can lead to dissimilar responses using the same hydrological model). We computed the Nash–Sutcliffe (N–S) coefficient, the Modified Efficiency Coefficient (MCE) (Legates and McCabe, 1999) and the determination coefficient ($R^2$) to compare $W_{post\text{-}s}(x)$ to $W_{pre\text{-}s}(x)$. Values for these coefficients distinct to one imply differences between both width functions, which also indicate that the terrain before and after the segmentation might also differ hydrologically. In this case both width functions particularly differ at the upper zone of the basin (i.e. distance between 4400 and 6000 m from the outlet in Fig. 13a). This difference is strongly associated with the segmentation process, which affects areas located at initial portions of the flow paths.

Spectral analysis is a useful tool to study the width function in more details and get information about its structure in the frequency domain (Rodriguez-Iturbe and Rinaldo, 1997; Richards-Pecou, 2002; Moussa, 2008). Thus, we further assessed the differences between $W_{pre\text{-}s}(x)$ to $W_{post\text{-}s}(x)$ by comparing the cross-spectral power density between $W_{pre\text{-}s}(x)$ and $W_{post\text{-}s}(x)$ (i.e. the power spectral of cross-covariance of the two functions represented by $P_{xy}2$ Fig. 13b), and the power spectral density of $W_{pre\text{-}s}(x)$ (represented by $P_{xy}1$ Fig. 13b). These functions were computed using algorithms embedded in Matlab®. Results demonstrated a significant similitude between $W_{pre\text{-}s}(x)$ and $W_{post\text{-}s}(x)$ at low frequencies, but more noticeable differences at higher frequencies. Thus, large scales features in both cases are very similar (i.e. total area, overall topography and shape, and main channel network structure, etc.), whereas particular features at frequencies higher than $0.3/20\ \mathrm{m}^{-1} = 1/66\ \mathrm{m}^{-1}$ are different (i.e. spatial scales smaller than 66 m). The real implications of the differences at these scales between $W_{pre\text{-}s}(x)$ and $W_{post\text{-}s}(x)$ in the simulated hydrologic response should be further studied using a hydrologic model, although noticeable impacts at very small scales are expected. It is also worth noticing that previous studies have concluded that high-frequency components of $W(x)$ may be useful for classification of river network topology and the regionalization of floods (Richards-Pecou, 2002; Lashermes and Foufoula-Georgiou, 2007, Moussa, 2008). Finally, and in addition to the hydrologic modeling, in-situ experimental facilities also provide valuable data. In that sense, a dense limnimeter network,

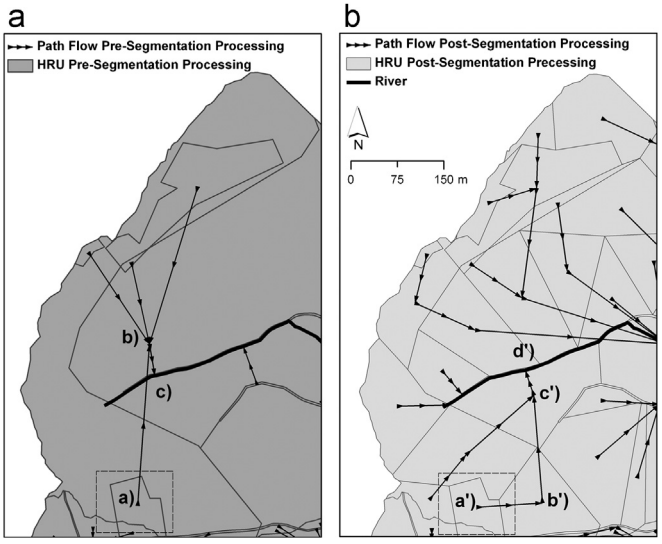


**Fig. 12.** Generated overland flow paths in the Mercier Catchment: (a) pre-segmented mesh, (b) post-segmented mesh.

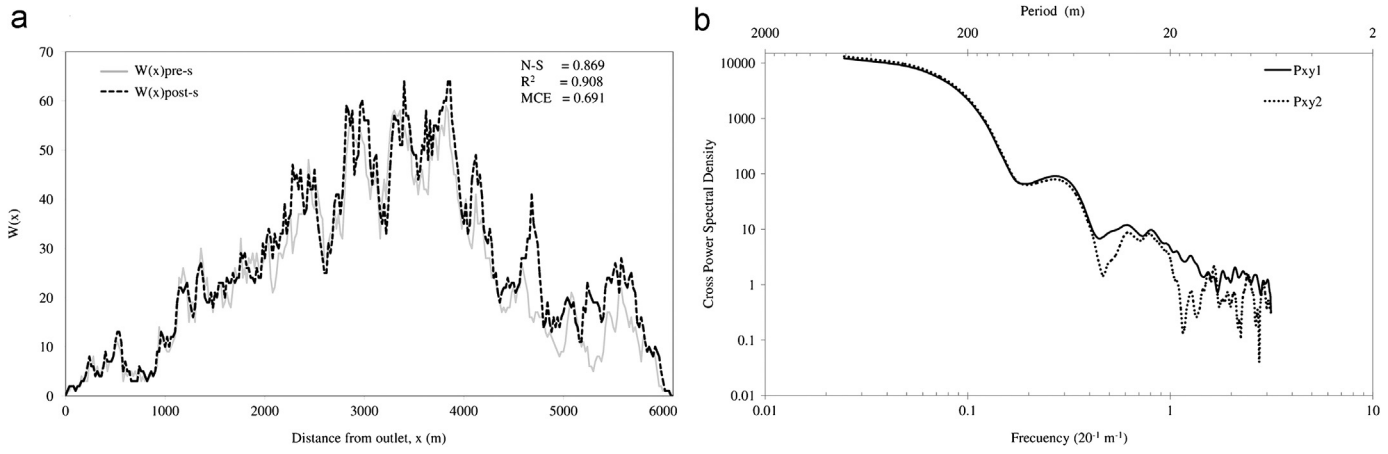


**Fig. 13.** (a) Width function $W(x)$ of Mercier Drainage Network for the pre- and post-segmentation (b) Power spectral density of Wpre-s($x$), $Pxy1$, and cross-spectral power density between Wpre-s($x$) and Wpost-s($x$), $Pxy2$.

recently implemented in the Mercier catchment (Sarrazin, 2012), will add valuable information to our results, and help to better understand local hydrological features at these small scales.

## 5. Conclusions and perspectives

In this study we proposed and tested various mesh generation tools implemented in GRASS-GIS to improve the HRUs representation used by distributed hydrological models. HRUs can be irregular and numerous for small to medium size catchments, making the computer-assisted pre-processing necessary. The developed algorithms address the following issues to obtain more regular and physically meaningful HRUs:

- *High heterogeneity in geometric/morphologic properties within the HRUs*. We proposed new algorithms for segmentation of units based on DEM-properties, which lead to polygons in which the property is more homogeneous, and therefore more suitable for hydrologic modeling.
- *Bad shaped polygons*. We found that the convexity index was relevant when identifying bad-shaped polygons. These were corrected using a triangulation/dissolution process oriented to increase the convexity index to a value larger than a critical value of 0.75, which we recommended for simple meshes, and 0.88 for detailed meshes.
- *Very large polygons that transfer large volumes of water into very small units, which can alter the calculation of flow paths, water fluxes and ponding levels*. We adopted the segmentation process based on the convexity criterion and a maximum triangular area.

Our treatments lead to significant changes both in the extension and trajectory of the overland flow paths. We assessed these changes by comparing the width function before and after processing the mesh representing the terrain. Because of the linkage between this function and the hydrologic response, we concluded that the segmentation processes can impact to some extent in the simulated hydrographs when using a hydrologic model.

Potential directions for future research include (1) generalization and improvement of the sequence in which the mesh segmentation's routines are implemented in order to reduce computation time; (2) implementation of a smoothing process algorithm prior to segmentation to simplify the representation of highly complex polygons in which computation time is very intensive (e.g. polygons created when forest/vegetation representation is too fine); (3) application of the raster property segmentation script with the altitude as the criterion given for its effect on flow routing; (4) corrections of long and thin HRUs (e.g. roads and hedgerows) by segmentation based on the compact index, as these polygons can act as artificial walls distorting the definition of overland flow paths, despite their high convexity; and (5) use of a hydrologic model to better assess the impacts of the different terrain representations and the segmentation process here proposed on the hydrologic simulation.

## Acknowledgments

AVuPUR project funded by the French National Research Agency (contract ANR-07-VULN-01) is acknowledged. Data were provided by CCVL, IGN, Grand Lyon, Météo-France, Nantes-Métropole, SAGYRC, SIAVHY, and Sol-Info Rhône-Alpes. SPOT images were acquired thanks to an ISIS contract. We also thank Grant no. 11090136 from the Chilean FONDECYT program, financial supports from Irstea-Lyon, through the EGIDE Association, and the Academic Department of University of Chile through its Program of Short Internships.

## Appendix A1. Raster-property segmentation script

1. Extract the raster property with the polygon mask.
2. Get property statistics for each polygon (average, standard deviation) (Fig. 3a).
3. If $\sigma > \sigma_T$.
4. Get Q1 and Q3 quartile values in the raster map.
5. Create Contour polylines with Q1 and Q3 values classification (Fig. 3b).
6. Dissolve small areas and preserve only the three largest areas (Fig. 3c).
7. Smooth Contours with Snakes Algorithm (Fig. 3d).
8. Reduce vertex Contours with Douglas–Peucker Algorithm (Fig. 3e).
9. Split Polygon with Q1 and Q3 contour polyline (Fig. 3f).

## Appendix A2. Convex segmentation script

```
1.- For each polygon P with CI ≤ ≤ CIT
2.-         Apply triangle
3.-         While P has triangles not yet dissolved
4.-                 Select triangle with the largest area
5.-                 Select triangle neighbor with the largest area
  and create new group P′
6.-                   While C. I. of P′ ≥ ≥ CIT
7.-                         Search the neighbor triangles with the
  largest area
8.-                         Dissolve boundaries of this group
9.-                          Compute the CI of this new group
10.-                         end while
11.-              Update P=P–P′
12.-        end While
13.-        Dissolve areas < area threshold
14.- end For
```

## References

Abbott, M.B., Bathurst, J.C., Cunge, J.A., O'Conell, P.E., Rasmusson, J., 1986a. An introduction to the European Hydrological System—Système Hydrologique Européen, "SHE", 1: History and philosophy of a physically-based distributed modeling system. Journal of Hydrology 87, 45–59.

Abbott, M.B., Bathurst, J.C., Cunge, J.A., O'Connell, P.E., Rasmussen, J., 1986b. An introduction to the European hydrological system—Système Hydrologique Européen "SHE". 2: Structure of a physically-based distributed modeling system. Journal of Hydrology 87, 61–77.

Arnold, J.G., Srinivasan, R., Muttiah, R.S., Williams, J.R., 1998. Large area hydrologic modeling and assessment Part I: Model development. Journal of the American Water Resources Association 34, 73–89.

Beven, K., Kirkby, M.J., 1979. A physically-based variable contributing area model of basin hydrology. Hydrological Sciences Bulletin 24, 43–69.

Bongartz, K., 2003. Applying different spatial distribution and modeling concepts in three nested mesoscale catchments of Germany. Physics and Chemistry of the Earth, Parts A/B/C 28, 1343–1349.

Branger, F., Braud, I., Debionne, S., Viallet, P., Dehotin, J., Hénine, H., Nédélec, Y., Anquetin, S., 2010. Towards multi-scale integrated hydrological models using the LIQUID framework. Overview of the concepts and first application examples. Environmental Modeling and Software 25, 1672–1681.

Branger, F., Jankowfsky, S., Vannier, O., Viallet, P., Debionne, S., Braud, I., 2012. Use of open-source GIS and data base software for the pre-processing of

distributed hydrological models. In: Bocher, E., Neteler, M. (Eds.), Geospatial Free and Open Source Software in The 21rst Century, Lecture notes in Geoinformation and Cartography. Springer, Berlin, pp. 35–48.
Braud, I., Breil, P., Thollet, F., Lafouy, M., Branger, F., Jacqueminet, C., Kermadi, S., Michel, K., 2013. Evidence of the impact of urbanization on the hydrological regime of a medium-sized periurban catchment in France. Journal of Hydrology 485, 5–23, http://dx.doi.org/10.1016/j.jhydrol.2012.04.049.
BRGM, 2013. Bureau of Geological and Mining Research. URL: 〈http://infoterre.brgm.fr/viewer/MainTileForward.do;jsessionid=C6247604415C79ABC472956-3FD5969E〉, (In French, accessed 29.01.13).
Bocher, E., Martin, J.Y., 2012. TAnaTo2: A tool to evaluate the impact of natural and anthropogenic artefacts with a TIN-based model. In: Bocher, E., Neteler, M. (Eds.), Geospatial Free and Open Source Software in the 21st Century, Lecture notes in Geoinformation and Cartography. Springer, Berlin, pp. 63–85.
Brossard, F., 2011. Automatisation du prétraitement des données spatiales pour la modélisation hydrologique distribuée en zone péri-urbaine (Automatic pre-processing of spatial data for a distributed hydrological modeling in a peri-urban zone). Rapport de Stage 2AE. EPMI École D'Ingenieurs. Cemagref-Lyon, vol. 77, (in French).
CGAL, 2011. Computational Geometry Algorithms Library (CGAL). URL: 〈www.cgal.org〉 (accessed 29.01.13).
Dehotin, J., Braud, I., 2008. Which spatial discretization for distributed hydrological models? Proposition of a methodology and illustration for medium to large scale catchments. Hydrology and Earth System Sciences 12, 769–796.
Di Luzio, M., Srinivasan, R., Arnold, J.G., 2004. A GIS-coupled hydrological model system for the watershed assessment of agricultural nonpoint and point sources of pollution. Transactions in GIS 8, 113–136.
Douglas, D.H., Peucker, T.K., 1973. Algorithms for the reduction of the number of points required to represent a digitized line or its caricature. Cartographica: The International Journal for Geographic Information and Geovisualization 10, 112–122.
Flügel, W.A., 1995. Delineating hydrological response units by geographical information system analyses for regional hydrological modeling using PRMS/MMS in the drainage basin of the River Bröl, Germany. Hydrological Processes 9, 423–436.
Garbrecht, J., Martz, L.W., 1997. TOPAZ version 1.20: An Automated Digital Landscape Analysis Tool for Topographic Evaluation, Drainage Identification, Watershed Segmentation and Subcatchments Parametrization—Overview. Report # GRL 97-2. Grazinglands Research Laboratory, USDA. Agricultural Research Service, El Reno, OK, 21 pp.
Gironás, J., Andrieu, H., Roesner, L., 2007. Alterations to Natural Catchments due to Urbanization. A Morphologic Approach. Novatech 2007. Section 6.2. GRAIE, Lyon, France, pp. 1199–1206.
Gironás, J., Niemann, J.D., Roesner, L.A., Rodriguez, F., Andrieu, H., 2009. A morpho-climatic instantaneous unit hydrograph model for urban catchments based on the kinematic wave approximation. Journal of Hydrology 377, 317–334.
Gironás, J., Niemann, J.D., Roesner, L.A., Rodriguez, F., Andrieu, H., 2010. Evaluation of methods for representing urban terrain in stormwater modeling. Journal of Hydrologic Engineering 15, 1–14.
GRASS Development Team, 2011. Geographic Resources Analysis Support System (GRASS) Software. Open Source Geospatial Foundation Project. URL: 〈http://grass.osgeo.org〉 (accessed 29.01.13).
Greene, D., 1983. The decomposition of polygons into convex parts. Computational Geometry 1, 235–259.
Hertel, S., Mehlhorn, K., 1983. Fast triangulation of simple polygons. In: Karpinski, M. (Eds). Proceedings of 4th International Conference Foundations Computation Theory. Lecture Notes in Computer Science, vol. 158, pp. 207–218.
Hofierka, J., Mitasova, H., Neteler, M., 2007. Terrain parameterization in GRASS. In Geomorphometry. In: Hengl, T., Reuter, H.I. (Eds.), Geomorphometry: Concepts, Software, Applications. Developments in Soil Science, vol. 33. Elsevier, pp. 1–28.
IGCS, 2013. Inventaire et Gestion des Sols. 〈http://www.gissol.fr/programme/igcs/rrp.php〉 (accessed 30.01.13).
Ivanov, V.Y., Vivoni, E.R., Bras, R.L., Entekhabi, D., 2004. Catchment hydrologic response with a fully distributed triangulated irregular network model. Water Resource Research 40, W11102, http://dx.doi.org/10.1029/2004WR003218.
Jacqueminet, C., Kermadi, S., Michel, K., Béal, D., Branger, F., Jankowsky, S., Braud, I., 2013. Land cover mapping using aerial and VHR satellite images for distributed hydrological modelling of periurban catchments: Application to the Yzeron catchment (Lyon, France). Journal of Hydrology 485, 68-83. http://dx.doi.org/10.1016/j.jhydrol.2013.01.028.
Jankowfsky, S., Branger, F., Braud, I., Debionne, S., Viallet, P., Rodriguez, F., 2010. Development of a suburban catchment model within the LIQUID® framework. In: Proceedings of the International congress on Environmental Modeling and Software. iEMSs 2010, Ontario, Ottawa, Canada, pp. 9.
Jankowfsky, S., Branger, F., Braud, I., Grionás, J., Rodriguez, F. Comparison of catchment and network delineation approaches in complex suburban environments: application to the Chaudanne catchment, France. Hydrological Processes, http://dx.doi.org/10.1002/hyp.9506.
Jankowfsky, S., 2011. Understanding and modeling of hydrological processes in small peri-urban catchments using an object oriented and modular distributed approach. Application to the Chaudanne and Mercier sub-catchments (Yzeron Catchment, France). École Doctorale Terre, Univers, Environnement. l'Institut National Polytechnique de Grenoble. URL: 〈http://tel.archives-ouvertes.fr/tel-00721988〉 (accessed 29.01.13).
Kass, M., Witkin, A., Terzopoulos, D., 1988. Snakes: active contour models. International Journal of Computer Vision 1, 321–331.
Klingseisen, B., Metternicht, G., Paulus, G., 2008. Geomorphometric landscape analysis using a semi-automated GIS-approach. Environmental Modeling and Software 23 (1), 109–121.
Krause, P., 2002. Quantifying the impact of land use changes on the water balance of large catchments using the J2000 model. Physics and Chemistry of the Earth 27, 663–673.
Lashermes, B., Foufoula-Georgiou, E., 2007. Area and width functions of river networks: new results on multifractal properties. Water Resources Research 43, W09405, http://dx.doi.org/10.1029/2006WR005329.
Lagacherie, P., Rabotin, M., Colin, F., Moussa, R., Voltz, M., 2010. Geo-MHYDAS: a landscape discretization tool for distributed hydrological modeling of cultivated areas. Computers and Geosciences 36, 1021–1032.
Legates, D.R., McCabe Jr., G.J., 1999. Evaluating the use of "goodness-of-fit" measures in hydrologic and hydroclimatic model validation. Water Resources Research 35, 233–241, http://dx.doi.org/10.1029/1998WR900018.
Lhomme, J., Bouvier, C., Perrin, J.L., 2004. Applying a GIS-based geomorphological routing model in urban catchments. Journal of Hydrology 299 (3–4), 203–216.
Meierdiercks, K.L., Smith, J.A., Baeck, M.L., Miller, A.J., 2010. Analyses of urban drainage network structure and its impact on hydrologic response. Journal of the American Water Resources Association 46, 932–943.
Moussa, R., 2008. What controls the width function shape, and can it be used for channel network comparison and regionalization? Water Resources Research 44, W08456, http://dx.doi.org/10.1029/2007WR006118.
Moussa, R., Voltz, M., Andrieux, P., 2002. Effects of the spatial organization of agricultural management on the hydrological behaviour of a farmed catchment during flood events. Hydrological Processes 16, 393–412.
Ogden, F.L., Raj Pradhan, N., Downer, C.W., Zahner, J.A., 2011. Relative importance of impervious area, drainage density, width function, and subsurface storm drainage on flood runoff from an urbanized catchment. Water Resources Research 47, W12503, http://dx.doi.org/10.1029/2011WR010550.
Olivera, F., Furnans, J., Maidment, D.R., Djokic, D., Ye, Z., 2002. Drainage Systems. Arc Hydro, GIS for Water Resources. D. R. Maidment, (Ed.), ESRI. Redlands, Ca, pp. 55–86.
O'Rourke, J., 1998. Computational Geometry in C, 2nd edition Cambridge University Press, Cambridge, England 376 pp.
Python Software Foundation, 2011. Python Programming Language—Official Website. URL: 〈www.python.org〉 (accessed 29.01.13).
R Development Core Team, 2011. R: A language and environment for statistical computing. R Foundation for Statistical Computing, Vienna, Austria. URL: 〈http://www.R-project.org/〉 (accessed 29.01.13).
Rabotin M., 2010. General Manual GeoMhydas. Laboratory of Interactions Soil–Agrosystem–Hydrosytem (LISAH), Montpellier, France. URL: 〈http://www.umr-lisah.fr/openfluid/index.php?page=dloadsmhy&lang=en&part=mhydas〉 (accessed 29.01.13).
Richards-Pecou, B., 2002. Scale invariance analysis of channel network width function and possible implications for flood behaviour. Hydrological Sciences Journal 47 (3), 387–404.
Rodriguez, F., Andrieu, H., Creutin, J., 2003. Surface runoff in urban catchments: morphological identification of unit hydrographs from urban databanks. Journal of Hydrology 283, 146–168.
Rodriguez, F., Cudennec, C., Andrieu, H., 2005. Application of morphological approaches to determine unit hydrographs of urban catchments. Hydrological Processes 19 (5), 1021–1035.
Rodriguez, F., Bocher, E., Chancibault, K., 2012. Terrain representation impact on periurban catchment morphological properties, Journal of Hydrology. http://dx.doi.org/10.1016/j.jhydrol.2012.11.023, in press.
Rodriguez-Iturbe, I., Rinaldo, A., 1997. Fractal River Basins: Chance and Self-organization. Cambridge University Press, New York 564 pp.
Russ, J.C., 2002. The Image Processing Handbook, Fourth edition CRC Press, Boca Raton, EUA 732 pp.
Sarrazin, B., 2012. MNT et observations multi-locales du réseau hydrogranphique d'un petit bassin versant rural dans une perspective d'aide à la modélisation hydrologique. (DTM and local observations of the river network of a small rural catchment with a view to support hydrological modeling). Ph.D. Dissertation. École Doctorale Terre, Univers, Environnement. l'Institut National Polytechnique de Grenoble, 275 pp (in French).
Seyfried, M., Wilcox, B., 1995. Scale and the nature of spatial variability: field examples having implications for hydrologic modeling. Water Resources Research 31, 173–184.
Schwartze, C., 2008. Deriving Hydrological Response Units (HRUs) using a Web Processing Service implementation based on GRASS-GIS. In: Geoinformatics FCE CTU 2008. Workshop Proceedings, vol. 3, pp. 67–78.
Shewchuck J., 1996. Triangle: Engineering a 2D Quality Mesh Generator and Delaunay Triangulator. In: Lin, M., Manocha, D., (Eds), Applied Computational Geometry: Towards Geometric Engineering, vol. 1148, pp. 203–222.
Smith, J., Lynn, M., Morrison, J., Sturdevant-Rees, P., Turner-Guillespie, D., Bates, P., 2001. The regional hydrology of extreme floods in an urbanizing drainage basin. Journal of Hydrometeorology 3, 267–282.
Taylor, J.A., Coulouma, G., Lagacherie, P., Tisseyre, B., 2009. Mapping soil units within a vineyard using statistics associated with high-resolution apparent soil electrical conductivity data and factorial discriminant analysis. Geoderma 153 (1–2), 278–284.

VanderKwaak, J.E., Loague, K., 2001. Hydrologic-response simulations for the R-5 catchment with a comprehensive physics-based model. Water Resources Research 37 (4), 999–1013.
Viviroli, D., Zappa, M., Gurtz, J., Weingartner, R., 2009. An introduction to the hydrological modeling system PREVAH and its pre- and post-processing tools. Environmental Modeling and Software 24, 1209–1222.
Wolock, D.M., Price, C.V., 1994. Effects of digital elevation model map scale and data resolution on a topography-based watershed model. Water Resource Research 30, 3041–3052.
Zhang, W., Montgomery, D., 1994. Digital elevation model grid size, landscape representation, and hydrologic simulations. Water Resource Research 30, 1019–1028.